Two-Photon Excitation and Optical Spatial-Profile Reshaping via a Nonlinear Absorbing Medium†

Guang S. He, Jacek Swiatkiewicz, Yan Jiang, and Paras N. Prasad*

Photonics Research Laboratory, Department of Chemistry, State University of New York at Buffalo, Buffalo, New York 14260-3000

Bruce A. Reinhardt and Loon-Seng Tan

Polymer Branch, Materials Directorate, United States Air Force Research Laboratory, Wright-Patterson Air Force Base, Dayton, Ohio 45433-7750

Ramamurthi Kannan

Systran Corporation, Dayton, Ohio 45432

Received: January 31, 2000

Two-photon processes have recently received considerable attention, as they offer opportunities for both fundamental research and technological applications. In this paper, we illustrate both of these opportunities by reporting on a study of two-photon properties and discussing one specific application of a new chromophore, tris[4-(7-benzothiazol-2-yl-9,9-diethylfluoren-2-yl)phenyl]amine (AF-350). This new compound exhibits a large two-photon absorptive cross section and, more importantly from the application point of view, a high photochemical/photothermal stability. The nonlinear optical properties of an AF-350 solution were studied with ∼800-nm laser pulses in both nanosecond and femtosecond regimes. The two-photon excited fluorescence spectrum and temporal behavior were compared with the corresponding results obtained for one-photon excitation. There is an ∼11-ps delay between an ultrashort pump pulse and the first peak of the two-photon induced fluorescence signal, whereas no delay was measured between the pump pulse and the first peak of the one-photon induced fluorescence. The measured effective two-photon absorption (TPA) cross section is $\sigma_2 = (151 \pm 23) \times 10^{-20}$ cm^4/GW for 7-ns, 810-nm laser pulses and $\sigma_2 = (0.61 \pm 0.02) \times 10^{-20}$ cm^4/GW for 135-fs, 796-nm laser pulses. One specific application reported here is the spatial-profile reshaping and smoothing of a focused laser field.

1. Introduction

Two-photon processes, perceived until recently to be of only academic interest, are now receiving a great deal of interest for their many potential technological applications.[1−16] This area offers numerous opportunities both for fundamental research and for new application development. From the fundamental research point of view, there are numerous challenges for computational chemists. Some of these are (i) developing a fundamental understanding of the structure−property relationship for efficient two-photon excitation; (ii) achieving an understanding of cooperative enhancement of two-photon absorption in a multibranch structure, which has recently been observed;[17] and (iii) devising a means of predicting the dynamics of two-photon excited states, such as the two-photon excited configuration and excited-state absorption.

In this paper, we present the two-photon properties of a newly synthesized organic chromophore that exhibits a strong two-photon absorption (TPA). To determine the role of excited-state absorption, we make the measurements with both nanosecond and femtosecond laser pulses. It has already been established by time-resolved measurements that the excited-state absorption originating from the two-photon excited state may provide a dominant contribution when longer (nanosecond) laser pulses are used.[18]

Using a streak camera, we obtain information on the buildup and decay of the upconverted fluorescence, helping us to identify whether the fluorescence originates directly from the two-photon excited state or from another state subsequently populated.

Finally, on the basis of a 1-cm path-length solution sample of this chromophore, a technological application for optical spatial-profile reshaping is demonstrated, perhaps for the first time, with a 7-ns, 810-nm laser beam passing through that sample.

2. Molecular Design and Chemical Structure

The organic chromophore used in the present work is tris-[4-(7-benzothiazol-2-yl-9,9-diethylfluoren-2-yl)phenyl]amine (AF-350), recently synthesized at the Polymer Branch of the Air Force Research Laboratory at Dayton, OH.

Two general organic structural types for two-photon-absorbing dyes were considered and prepared in our initial study.[19] Type-I chromophores are symmetrical compounds, with 2-benzothiazolyl groups as electron acceptors and electron-rich thiophene or 2,2′-bithiophene groups acting as both donors and a polarizable π-bridge. Type-II chromophores are unsymmetrical

† Part of the special issue "Electronic and Nonlinear Optical Materials: Theory and Modeling".

10.1021/jp000370+ CCC: $19.00
Published on Web 04/25/2000

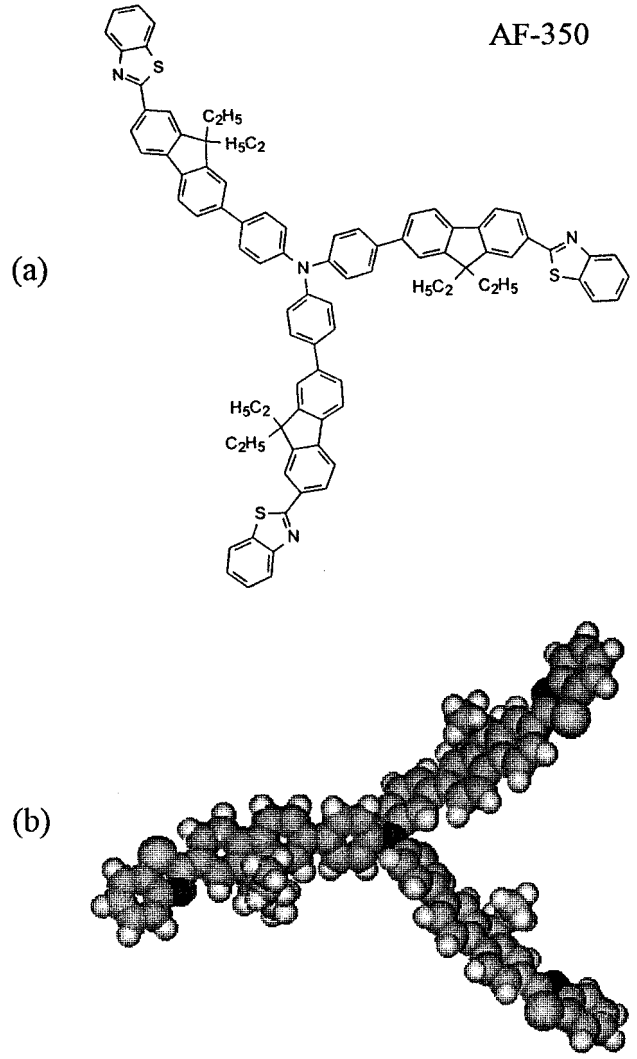

Figure 1. (a) Molecular structure and (b) top view of computer simulated three-dimensional picture of AF-350.

compounds having a generic D−π−A structural motif, composed of a diarylamine donor, a fluorene π-bridge, and a pyridine acceptor. The latter class of compounds, in general, has better TPA cross sections than the former. However, other researchers have found symmetrical compounds with structural motifs such as D−π−A and D−π−A−π−D, where D = tertiary amine donors[11] and α,ω-dithienylpolyenes,[20] to be good TPA materials. These are linearly symmetric compounds similar to our type-I chromophores.

Following the success of our initial work, we are particularly interested in further improving the TPA cross section by increasing the effective conjugation length without shifting the TPA peak away from our measurement wavelength of ~800 nm. Conjugation through nitrogen seemed to be a good strategy. This conclusion was supported by the molecular simulation result and by the UV−vis spectroscopic observation that, in the triphenylamine-based oligo(arylenevinylene), the central, tertiary nitrogen atom does not interrupt the conjugation between the two vinyl groups.[21] In addition, another advantage to using triarylamine as the central unit is that it also provides two-dimensional conjugation. On the basis of these considerations, we designed and synthesized the AF-350 compound. The molecular structure and the corresponding space-filling, three-dimensional rendition of AF-350 are depicted in Figure 1. In obtaining the molecular three-dimensional illustration, we used HyperChem software version 5.1 and the Polak-Ribiere method

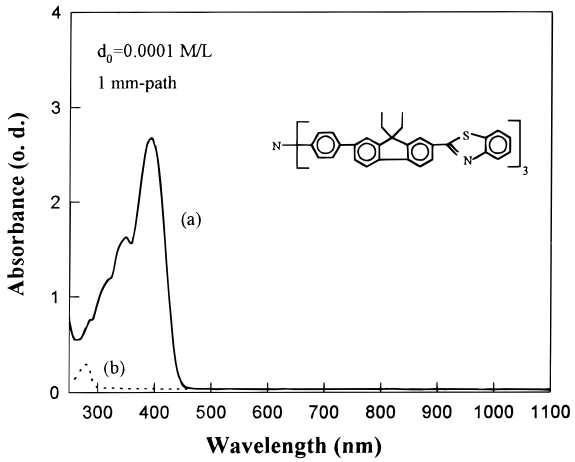

Figure 2. Linear absorption spectra of (a) an AF-350 solution in THF at a concentration of $d_0 = 0.0001$ M and (b) a pure THF sample. The path length of the sample was 1 mm.

as the energy minimization algorithm. Three features are evident from the molecular structure of AF-350. (i) Each of the three arms connected to the central nitrogen atom is nearly planar. (ii) The bond angles around the central nitrogen atom are very close to the idealized value for an sp^2-hybridized nitrogen atom (i.e., 120°). (iii) The dihedral (torsion) angles between adjacent arms, as indicated by the degrees of tilting of one phenyl ring from the other connected to the central nitrogen atom, are ~43.4°. These features suggest that conjugation does spread over the entire molecule and that the presence of the central nitrogen atom does not block conjugation between any two arms.

3. Spectra and Temporal Behavior of One- and Two-Photon Induced Fluorescence

Figure 2 shows the linear absorption spectrum of a 1-mm path-length AF-350 solution in tetrahydrofuran (THF) with a solute concentration of $d_0 = 0.0001$ M, obtained with a scanning spectrophotometer (UV-3101PC from Shimadzu). The linear absorption contribution from the same 1-mm path-length pure solvent sample is also shown in Figure 2 by a dotted line. One can see that there is a broad and strong absorption band with the peak wavelength located at ~400 nm, which is attributed to the AF-350 molecule. There is no linear absorption for the AF-350 solution in the spectral range from ~460 to ~1100 nm. However, the two-photon energy of near-IR radiation between ~700 and ~850 nm falls in the strong linear absorption bands of the AF-350 solution. We observe a strong frequency-upconverted fluorescence emission from an AF-350 solution with a moderate concentration when excited even with an unfocused near-IR pulsed laser beam at wavelengths in the range mentioned above. This implies a strong TPA process occurring within the solution sample.

Two laser systems were employed to investigate the two-photon induced fluorescence behavior of AF-350 solution samples: one was a 7-ns, 810-nm dye laser system pumped with a frequency-doubled Nd:YAG laser operating at 10 Hz and the other was a 135-fs, 796-nm Ti:sapphire oscillator/amplifier laser system operating at 1 kHz. The frequency-doubled output from these two laser systems (with wavelengths of 405 and 398 nm, respectively) was used to investigate the one-photon induced fluorescence behavior.

The measured spectra of one-photon and two-photon (in the nanosecond regime) induced fluorescence for the AF-350 solution in THF are shown in Figure 3, as recorded by a spectroflurophotometer (RF5000U from Shimadzu). The solu-

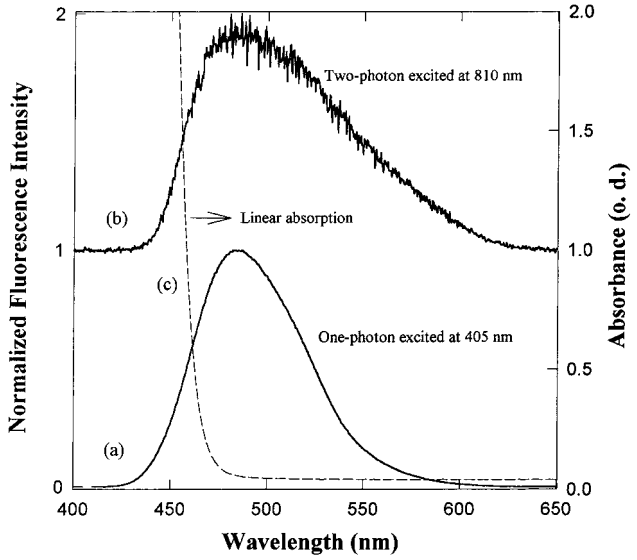

Figure 3. Normalized fluorescence spectra of an AF-350 solution excited by (a) one-photon absorption (at 405 nm) and (b) two-photon absorption (at 810 nm). The linear absorption of the 1-mm path-length, $d_0 = 0.033$ M solution sample is shown by the dashed curve (c).

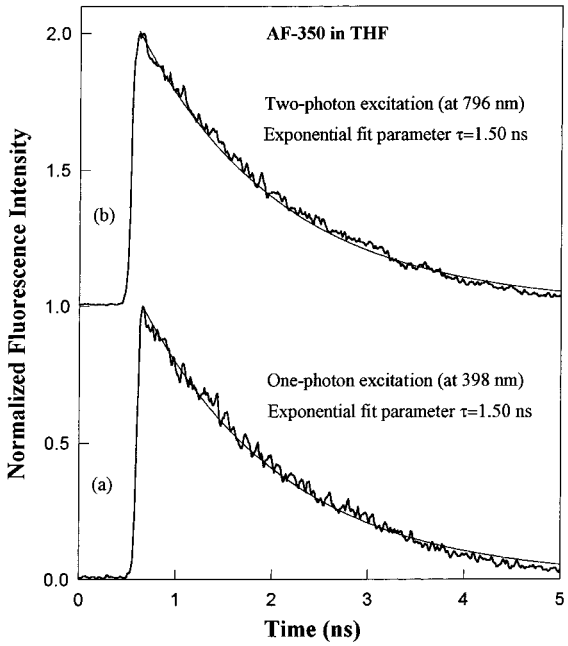

Figure 4. Normalized fluorescence decay curves of an AF-350 solution excited by (a) one-photon absorption (at 398 nm) and (b) two-photon absorption (at 796 nm).

tion sample of concentration $d_0 = 0.033$ M filled a 1-mm path-length quartz cuvette. In the same figure, the linear absorption edge on the long-wavelength side is shown by a dashed curve. It is shown in Figure 3 that the fluorescence spectra are basically the same for both the one-photon and the two-photon excitation cases, with the peak emission wavelength located at ~480 nm. Most of the emission wavelengths are away from the linear absorption band, i.e., there is a large Stokes shift.

The temporal behavior and lifetime of one-photon and two-photon induced fluorescence of the same AF-350 solution sample of concentration $d_0 = 0.033$ M were measured using a high-speed streak camera (C5680-22 from Hamamatsu). The measured fluorescence decay curves are shown in Figure 4 on a 5-ns full scale for one-photon and two-photon excitation (in the femtosecond regime). In both cases, the decay curves could

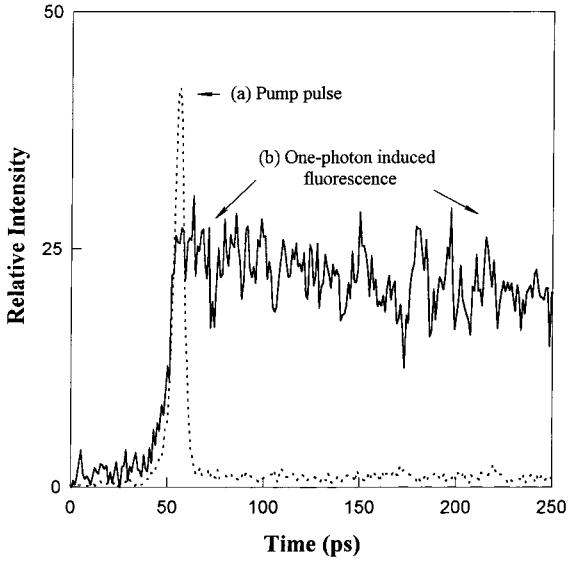

Figure 5. Temporal waveforms of (a) the ultrashort pump pulse (at 398 nm) and (b) the one-photon excited fluorescence signal.

be well fit by a single-exponential dependence with the same lifetime value of $\tau = 1.5 \pm 0.2$ ns (to decay to $1/e$ of the initial intensity).

On the basis of the facts that the emission spectra and the lifetimes of fluorescence are nearly the same for one-photon and two-photon excitations, one may conclude that, in both cases, the fluorescence emission is predominantly from the same state, the S_1 singlet band.[22,23] As there is a considerable Stokes shift between the pump wavelength λ_0 for one-photon excitation (or $\lambda_0/2$ for two-photon excitation) and the emission wavelengths, the excited molecules must relax to the lowest excited state of the S_1 singlet band before they start to emit the fluorescence. For this reason, there must be a definite time delay between the moments at which the absorption takes place and the emission starts. This delay time (Δt) can be measured if the pump pulse duration and the temporal resolution of the detection system are shorter than Δt. On the other hand, the upper states of the molecular transition for one-photon absorption and for two-photon absorption can be different. For example, in centrosymmetric structures, they are different because the one-photon excitation allows only $g \rightarrow u$ transitions, whereas the two-photon excitation produces a $g \rightarrow g$ transition. For this reason, the two-photon excitation/absorption spectra might be drastically different from the corresponding linear absorption spectra (in the absorbing photon-energy scale) for a given dye solution sample.[10,11,24−27] With these considerations in mind, one may expect that the measured delay time Δt might be different for one-photon and two-photon excitation processes. Our experimental results on the AF-350 solution have confirmed this expectation. Figure 5 shows the measured waveforms of the ultrashort pump pulse (398-nm) and the initial section of the one-photon induced fluorescence pulse, simultaneously recorded by the streak camera operating on a 500-ps full scale. We see that there is no observable delay between the pump pulse and the first burst of fluorescence emission. This observation implies that the molecular relaxation time of AF-350 from higher excited levels to the lowest level of the S_1 singlet band is $\Delta t \leq 3$ ps, which is the temporal uncertainty of our measurement system. In contrast, Figure 6 shows the pump pulse (796-nm) and two-photon induced fluorescence signal, from which we see an obvious delay ($\Delta t \approx 11$ ps) between the pump pulse and the first burst of the fluorescence. This result implies a much longer relaxation time of molecules from a

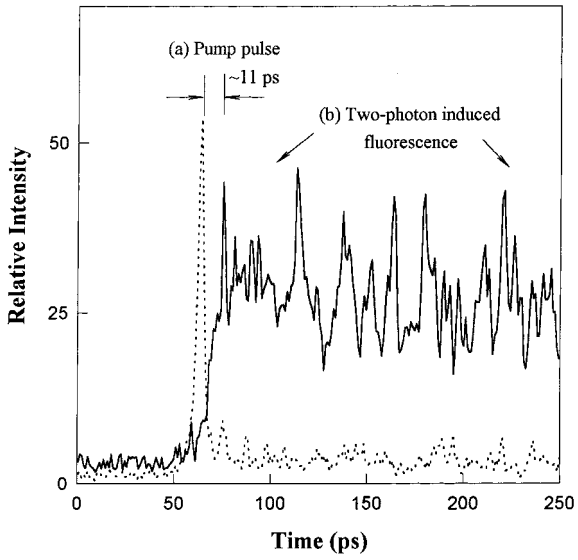

Figure 6. Temporal waveforms of (a) the ultrashort pump pulse (at 796 nm) and (b) the two-photon excited fluorescence signal.

higher two-photon excited state to the lowest excited state of the S_1 band. We believe that this is the first direct evidence to suggest that a one-photon excitation populates the S_1 level, whereas the two-photon excitation populates an S_2 level. In other words, even though the structure investigated here is unsymmetric, one-photon and two-photon excitations may lead to different states.[28−33] The observed ~11-ps delay corresponds to the time for the $S_2 \rightarrow S_1$ internal conversion.

4. TPA Cross Section and Optical Limiting Measurement

According to the basic consideration of the TPA process, the transmitted intensity of an intense light beam passed through a TPA medium can be expressed as[6]

$$I(x, L) = \frac{I(x, 0)}{1 + \beta L I(x, 0)} \tag{1}$$

where $I(x, 0)$ is the transverse intensity function of the input beam, x is the transverse variable in the beam section, L is the propagation distance in the medium, and β is the nonlinear absorption coefficient of the medium. If the beam is focused near the sample and if a Gaussian transverse distribution in the nonlinear medium can be assumed, the overall nonlinear transmissivity T_i will be[6]

$$T_i = [\ln(1 + I_0 L\beta)]/I_0 L\beta \tag{2}$$

where I_0 is the central intensity of the input beam with a Gaussian transverse distribution.

The experimental setup for nonlinear absorption measurements is the same as described previously in refs 8 and 9. A linearly polarized 7-ns, 810-nm, 10-Hz pulsed laser beam was chosen as the testing beam. After passing through a lens with a focal length of 20 cm, this laser beam was focused and passed through a 1-cm path-length quartz cuvette filled with the AF-350 solution of concentration $d_0 = 0.033$ M in THF. The position of the sample cell could be smoothly varied along the laser beam direction (z-axis), so that the local intensity within the 1-cm-thick sample cell could be changed under a constant total incident laser power level. The transmitted laser beam from the sample cell was then detected by an optical power meter with a larger detection area with an ~30-mm diameter. Thus,

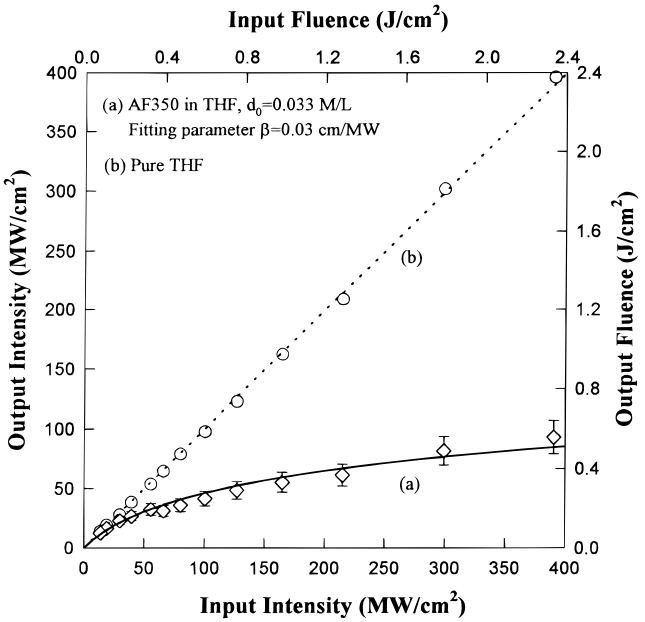

Figure 7. Measured output intensity (fluence) as a function of input intensity (fluence) based on (a) a 1-cm path-length AF-350 solution in THF of concentration $d_0 = 0.033$ M and (b) a 1-cm path-length pure THF sample. The solid line is the theoretical curve obtained with a fitting parameter of $\beta = 0.03$ cm/MW.

only the transmissivity change due to pure nonlinear absorption (not to the induced refractive index change) could be measured.

Figure 7 shows the measured output overall intensity (or fluence) of the 810-nm focused laser beam passed through a 1-cm-long AF-350 solution as a function of the input overall intensity (or fluence); the F-number of the focusing optics is 67. In comparison with the output/input curve obtained from a 1-cm-long pure THF sample, the data from the AF-350 solution sample showed us a superior optical limiting behavior: the nonlinear transmissivity decreased from ~0.92 to ~0.24 when the input beam intensity increased from ~10 to ~390 MW/cm^2. The solid-line curve in Figure 7 is the theoretical curve given by eq 2 with a best-fitting parameter $\beta = 0.03$ cm/MW. It is known that the nonlinear absorption coefficient is related to the molecular density N_0 (in units of cm^{-3}) and the TPA cross section σ_2 (in units of cm/GW) by[7]

$$\beta = \sigma_2 N_0 = \sigma_2 N_A d_0 \times 10^{-3} \tag{3}$$

where N_A (6.023×10^{23}) is Avogadro's number. For the AF-350 solution in THF, from the experimentally estimated value of $\beta = 0.03 \pm 0.0045$ cm/MW, we determine the value of the TPA cross section $\sigma_2 = (151 \pm 23) \times 10^{-20}$ cm^4/GW. This value is twice as large as that of another previously reported chromophore, AF-50.[8]

It is known that even for the same nonlinear absorbing medium, the measured effective TPA cross section can change greatly in different laser pulse-duration ranges.[10,11,18] We have conducted the TPA measurement for the same AF-350 solution in THF of concentration $d_0 = 0.033$ M using 135-fs, 796-nm, 1-kHz laser pulses from the Ti:sapphire laser system. An open-aperture Z scan was performed by moving a 1-mm cuvette containing the sample solution along the focused laser beam. The spatial beam distribution was confirmed to be a Gaussian shape with a Rayleigh range of ~4 mm. A large-diameter (12 mm) photodiode detector with appropriate neutral density filters was located behind the sample to measure intensity changes during the scan. The intensity of the laser beam at the sample

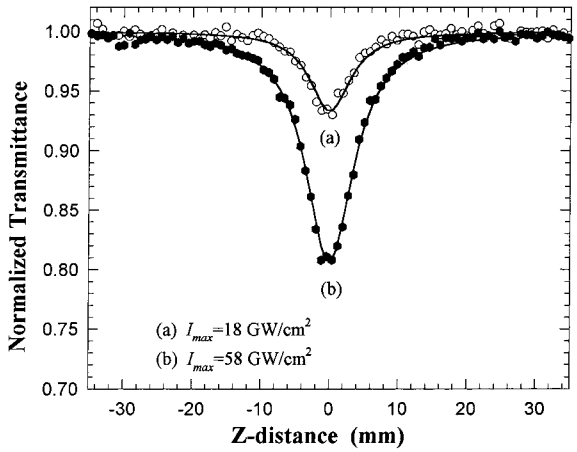

Figure 8. Measured transmittance of a 1-mm-thick AF-350 solution sample as a function of Z distance using 135-fs, 796-nm laser pulses at two different intensity levels in the focal-point position. The solid-line curves are obtained with a best-fitting parameter of $\sigma_2 = 0.61 \times 10^{-20}$ cm^4/GW.

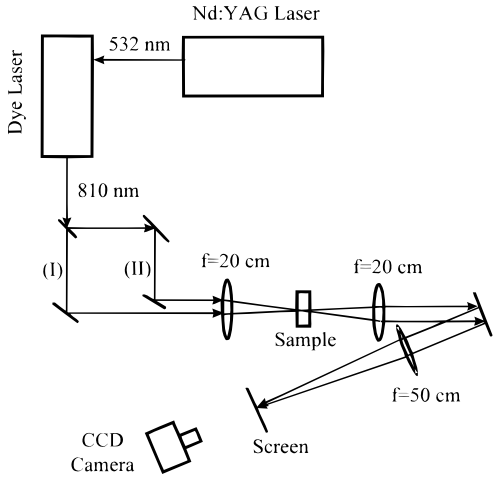

Figure 9. Experimental setup for generating a focused interference pattern inside the nonlinear medium and demonstrating the spatial-profile reshaping function.

was controlled with an attenuator and measured before the sample with a calibrated photodiode. Figure 8 shows the measured transmittance as a function of the Z distance from the focal point position at two different focal intensity levels. Both groups of experimental data can be well fit with an average value of the TPA cross section of $\sigma_2 = (0.61 \pm 0.02) \times 10^{-20}$ cm^4/GW. The difference between the values of the cross sections measured with the nanosecond and the femtosecond laser pulses suggests that, in the former case, the excited-state absorption may play an additional role for the observed effective nonlinear absorption.[10,11,18]

5. Optical-Field Reshaping via the AF-350 Solution

A TPA-based nonlinear medium can be highly useful not only for optical limiting, but also for reshaping of either the temporal profile or the spatial profile of an intense optical field.[34,35]

To examine the influence of nonlinear absorption on the spatial profile of the input laser field, a two-beam interference arrangement, shown schematically in Figure 9, was used to generate a quasi-periodic transverse intensity distribution around the focal plane or the center of the tested sample. After the 7-ns, 810-nm pulse passed through the sample, the change in its relative spatial profile could be measured with a far-field imaging lens system and a digital CCD camera system. Figure

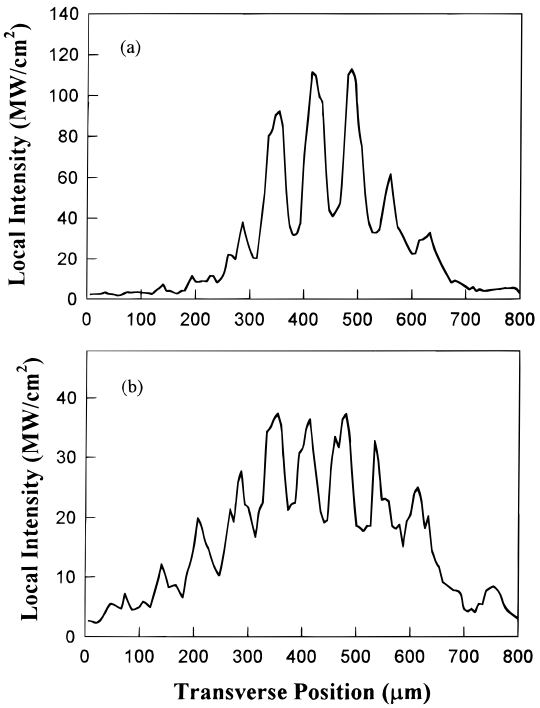

Figure 10. Measured transverse intensity distributions of the 810-nm laser beams passing through (a) a 1-cm path-length pure THF sample and (b) a 1-cm path-length AF-350 solution sample. The input focused intensity at the pattern center is ~113 MW/cm^2.

10a displays the measured focal transverse intensity distribution of the laser field after it passes through a 1-cm-long pure THF sample without any nonlinear absorption; it shows a nearly Gaussian shape envelope and a periodic spatial intensity modulation with the modulation depth of ~67%. Figure 10b presents the measured focal transverse intensity distribution of the same laser field after it passes through a 1-cm-long AF-350/THF solution sample of concentration $d_0 = 0.033$ M, which shows a much broader envelope and a smaller modulation depth (~39%). The changes in the spatial envelope and modulation depth of the focused laser beams in the nonlinear medium can be well understood by considering the dependence of nonlinear absorption on the local intensity, as described by eq 1 (or eq 2). To compare the experimental results with the theoretical results, Figure 11a shows an assumed input intensity distribution in the sample position, which is formed by a proper Gaussian function multiplied by an interference pattern function with a modulation depth of ~67%. Figure 11b illustrates the computer simulated spatial intensity distribution of the laser beams exciting the nonlinear medium, based on eq 2, with an assumed nonlinear absorption coefficient value of $\beta = 0.03$ cm/MW. Comparing Figure 11 to Figure 10, we see a reasonable agreement between the experimental results and the theoretical predictions based on the same β value. The TPA-based optical spatial-field reshaping effect can be especially useful for optical data processing, optical recognition, and optical spatial-field smoothing.

Finally, it should be noted that AF-350 in solution phase is highly stable. There is essentially no change in either the linear absorption spectrum or the value of the TPA cross section after 6 months of storage in an ambient-light environment and more than 50 h of measurement time using nanosecond and femtosecond laser pulses.

Acknowledgment. This work was supported by the Polymer Branch of the U.S. Air Force Research Laboratory and the U.S.

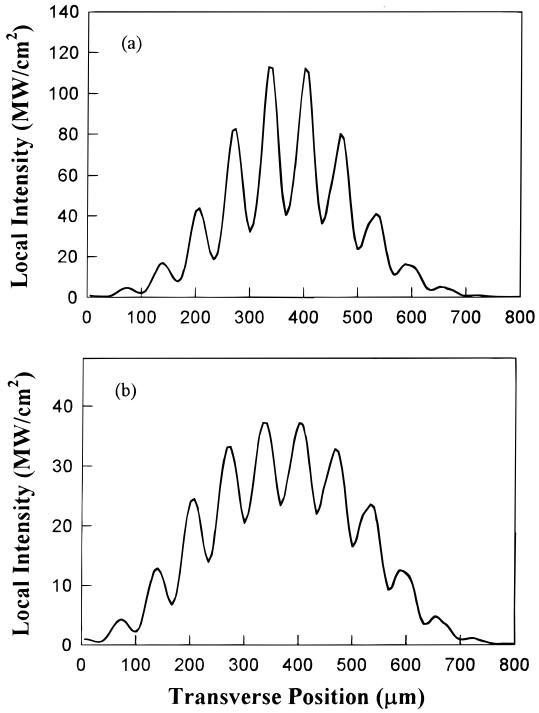

Figure 11. (a) Theoretically assumed input transverse intensity distribution and (b) computer-simulated output intensity distribution after the laser pulse passes through a nonlinear absorbing medium of $\beta = 0.03$ cm/MW.

Air Force Office of Scientific Research through Contract F4962093C0017.

References and Notes

(1) Parthenopoulos, D. A.; Rentzepis, P. M. *Science* **1989**, *245*, 843.
(2) Denk, W.; Strickler, J. H.; Webb, W. W. *Science* **1990**, *248*, 73.
(3) Bhawalkar, J. D.; He, G. S.; Prasad, P. N. *Rep. Prog. Phys*. **1996**, *59*, 1041.
(4) He, G. S.; Yuan, L.; Cui, Y.; Li, M.; Prasad, P. N. *J. Appl. Phys*. **1997**, *81*, 2529.
(5) He, G. S.; Bhawalkar, J. D.; Zhao, C. F.; Prasad, P. N. *IEEE J. Quantum Electron.* **1996**, *32*, 749.
(6) Tutt, L. W.; Boggess, T. F. *Prog. Quantum Electron*. **1993**, *17*, 299.
(7) He, G. S.; Xu, G. C.; Prasad, P. N.; Reinhardt, B. A.; Bhatt, J. C.; McKellar, R.; Dillard, A. G. *Opt. Lett*. **1995**, *20*, 435.
(8) He, G. S.; Yuan, L.; Cheng, N.; Bhawalkar, J. D.; Prasad, P. N.; Brott, L. L.; Clarson, S. J.; Reinhardt, B. A. *J. Opt. Soc. Am. B* **1997**, *14*, 1079.
(9) He, G. S.; Weder, C.; Smith, P.; Prasad, P. N. *IEEE J. Quantum Electron*. **1998**, *34*, 2279.
(10) Ehrlich, J. E.; Wu, X. L.; Lee, I.-Y. S.; Hu, Z.-Y.; Röckel, H.; Marder, S. R.; Perry, J. W. *Opt. Lett*. **1997**, *22*, 1843.
(11) Albota, M.; Beljonne, D.; Brédas, J.-L.; Ehrlich, J. E.; Fu, J.-Y.; Heikal, A. A.; Hess, S. E.; Kogej, T.; Levin, M. D.; Marder, S. R.; MaCord-Maughon, D.; Perry, J. W.; Röckel, H.; Rumi, M.; Subramaniam, C.; Webb, W. W.; Wu, X.-L.; Xu, C. *Science* **1998**, *281*, 1653.
(12) Dvormikov, A. S.; Rentzepis, P. M. *Opt. Commun*. **1997**, *136*, 1.
(13) Pudavar, H. E.; Joshi, M. P.; Prasad, P. N.; Reinhardt, B. A. *Appl. Phys. Lett*. **1999**, *74*, 1338.
(14) Bhawalkar, J. D.; Kumar, N. D.; Zhao, C. F.; Prasad, P. N. *J. Clin. Med. Surg*. **1997**, *37*, 510.
(15) Gura, T. *Science* **1997**, *276*, 1988.
(16) Bhawalkar, J. D.; Swiatkiewicz, J.; Prasad, P. N.; Pan, S. J.; Shin, A.; Samarabandu, J. K.; Cheng, P. C.; Reinhardt, B. A. *Polymer* **1997**, *38*, 4551.
(17) Chung, S.-J.; Kim, K.-S.; Lin, T.-C.; He, G. S.; Swiatkiewicz, J.; Prasad, P. N. *J. Phys. Chem. B* **1999**, *103*, 10741.
(18) Swiatkiewicz, J.; Prasad, P. N.; Reinhardt, B. A. *Opt. Commun*. **1998**, *157*, 135.
(19) Reinhardt, B. A.; Brott, L. L.; Clarson, S. J.; Dillard, A. G.; Bhatt, J. C.; Kannan, R.; Yuan, L.; He, G. S.; Prasad, P. N. *Chem. Mater*. **1998**, *10*, 1863.
(20) Spangler, C. W. *J. Mater. Chem*. **1999**, *9*, 2013.
(21) Sander, R.; Stümpflen, V.; Wendorff, J. H.; Greiner, A. *Macromolecules* **1996**, *29*, 7705.
(22) Duarte, F. J., Hillman, L. W., Eds. *Dye Laser Principles with Applications*; Academic Press: New York, 1990.
(23) Schäfer, F. P., Ed. *Dye Lasers*; Springer-Verlag: Berlin, 1990.
(24) Aslanidi, E. B.; Tikhonov, E. A. *Opt. Spectrosc*. **1974**, *37*, 446.
(25) Singer, L.; Baram, Z.; Ron, A.; Kimel, S. *Chem. Phys. Lett*. **1977**, *47*, 372.
(26) Smirnova, T. N.; Tikhonov, E. A.; Shpak, M. T. *JETP Lett*. **1979**, *29*, 411.
(27) Xu, C.; Webb, W. W. *J. Opt. Soc. Am. B* **1996**, *13*, 481.
(28) Drucker, R. P.; McClain, W. M. *J. Chem. Phys*. **1974**, *61*, 2616.
(29) Foucault, B.; Hermann, J. P. *Opt. Commun*. **1975**, *15*, 412.
(30) Fang, H. L. B.; Thrash, R. J.; Leroi, G. E. *J. Chem. Phys*. **1977**, *67*, 3389.
(31) Fuke, K.; Nagakura, S.; Kobayashi, T. *Chem. Phys. Lett*. **1975**, *31*, 205.
(32) Bergman, A.; Jortner, J. *Chem. Phys. Lett*. **1974**, *26*, 323.
(33) Bickel, G. A.; Innes, K. K. *J. Chem. Phys*. **1987**, *86*, 1752.
(34) He, G. S.; Yuan, L.; Bhawalkar, J. D.; Prasad, P. N. *Appl. Opt*. **1997**, *36*, 3387.
(35) He, G. S.; Guishi, R.; Prasad, P. N.; Reinhardt, B. A. *Opt. Commun.* **1995**, *117*, 133.